Published in final edited form as:
J Immunol. 2013 September 1; 191(5): 2474–2485. doi:10.4049/jimmunol.1202429.

Diet-induced obese mice exhibit altered heterologous immunity during a secondary 2009 pandemic H1N1 infection[1]

J. Justin Milner[*], **Patricia A. Sheridan**[*], **Erik A. Karlsson**[†], **Stacey Schultz-Cherry**[†], **Qing Shi**[*], and **Melinda A. Beck**[2,*]

[*]Department of Nutrition, Gillings School of Global Public Health, University of North Carolina at Chapel Hill, Chapel Hill, NC, USA

[†]Department of Infectious Diseases, St. Jude Children's Research Hospital Memphis, Memphis, TN, USA

Abstract

During the 2009 pandemic H1N1 (pH1N1) influenza outbreak, obese individuals were at greater risk for morbidity and mortality to pandemic infection. However, the mechanisms contributing to greater infection severity in obese individuals remain unclear. Although most individuals lacked pre-existing, neutralizing antibody protection to the novel pH1N1 virus, heterologous defenses conferred from exposure to circulating strains or vaccination have been shown to impart protection against pH1N1 infection in humans and mice. Because obese humans and mice have impaired memory T-cell and antibody responses following influenza vaccination or infection, we investigated the impact of obesity on heterologous protection to pH1N1 infection using a mouse model of diet-induced obesity. Lean and obese mice were infected with influenza A/PR/8/34 and five weeks later challenged with a lethal dose of heterologous pH1N1 (A/Cal/04/09). Cross-neutralizing antibody protection was absent in this model, but obese mice exhibited a significantly lower level of non-neutralizing, cross-reactive pH1N1 nucleoprotein antibodies following the primary PR/8 infection. Further, obese mice had elevated viral titers, greater lung inflammation, lung damage, and an increased number of cytotoxic memory $CD8^+$ T cells in the lung airways. Although obese mice had more regulatory T cells (Tregs) in the lung airways compared with lean controls during the pH1N1 challenge, Tregs isolated from obese mice were 40% less suppressive than Tregs isolated from lean mice. Taken together, excessive inflammatory responses to pH1N1 infection, potentially due to greater viral burden and impaired Treg function, may be a novel mechanism by which obesity contributes to greater pH1N1 severity.

Introduction

The novel 2009 pandemic H1N1 influenza A virus (pH1N1) is unique in several aspects. Despite causing greater disease severity in animal models compared to seasonal H1N1 strains (1–4), the pH1N1 virus caused relatively mild, uncomplicated symptoms in humans (5, 6). Further, in contrast to seasonal influenza epidemics, children and nonelderly adults were disproportionately susceptible to pH1N1 infection compared with elderly individuals (7, 8), with estimates that approximately 90% of pH1N1 deaths occurred in the nonelderly population (9). Clinical and epidemiological data suggest the lower susceptibly in

[1]This work was supported in part by NIH supported NORC DK56350, the NIH NIAID contract number HHSN266200700005C and the American Lebanese Syrian Associated Charities (ALSAC).

[2]Address correspondence and reprint requests to: Dr. Melinda A. Beck, Department of Nutrition, Gillings School of Global Public Health 2303 MHRC, CB No. 7461, University of North Carolina at Chapel Hill, Chapel Hill, NC 27599-7461. T:919-966-6809, F: 919-843-0776, melinda_beck@unc.edu.

individuals over 65 y of age is likely due to the presence of cross-reactive anti-hemagglutinin antibodies generated from previous exposure to pre-1950 influenza strains (8, 10–12). Because a majority of the population is naïve to these past circulating influenza strains, and recently circulating (pre-2009) seasonal strains and influenza vaccines did not elicit a robust cross-reactive antibody response, most individuals lacked neutralizing antibody protection against pH1N1 infection (10, 12–15).

Although antibodies are important for the control and even prevention of influenza infection, in their absence, influenza-specific T cells are essential in limiting influenza severity (16, 17). Several recent studies in animals and humans have demonstrated that previous exposure to seasonal influenza strains or vaccination can induce cross-reactive memory T cells that have the capacity to limit pH1N1 disease severity (15, 18–23). In mice, seasonal influenza viruses and vaccines elicit a memory T-cell response that can prevent morbidity and mortality to a lethal pH1N1 challenge (21, 24–27). Additionally, seasonal influenza A-specific memory T cells from humans (naïve to pH1N1) are capable of recognizing pH1N1 epitopes and can directly lyse pH1N1-infected target cells (19). Therefore, the ability of cross-protective memory T cells to control pH1N1 infection could explain the relatively benign symptoms experienced by a majority of those infected (19, 28). However, cross-reactive antibody protection to pH1N1 cannot be ignored. Non-neutralizing antibodies recognizing conserved epitopes, such as anti-nucleoprotein (NP) antibodies, have been shown to contribute heterologous protection to influenza infection, reducing viral titers and infection severity in mice (29, 30). Additionally, a primary seasonal infection can lead to an accelerated production of pH1N1 antibodies during a heterologous pH1N1 infection, which may facilitate pH1N1 viral clearance (25, 30).

Another novel characteristic of the pH1N1 virus is that obesity, defined as a BMI ≥ 30kg/m^2, was considered to be an independent risk factor for increased morbidity and mortality following infection (31–35). Obesity is a global public health concern, affecting more than one-in-ten of the world's adult population (36). It is well-established that obesity impacts several aspects of the immune response and increases susceptibility for a variety of pathogens, including influenza virus (37). Although recent investigations in mice and humans have begun to elucidate potential mechanisms by which obesity impairs anti-viral immunity to influenza infection, the specific factors contributing to the increased severity observed in the obese population remain unclear (37). We have previously demonstrated that obese mice and humans exhibit impaired memory $CD8^+$ T-cell responsiveness to influenza stimulation (38, 39). Further, obese mice display impaired responsiveness to influenza vaccination (40), and obese humans are unable to maintain long-term influenza antibody levels following vaccination (39). Therefore, given the protective nature of cross-reactive antibody and T-cell responses, we hypothesized that obesity impaired heterologous immunity induced by previous influenza exposure, resulting in greater pH1N1 infection severity.

In this study, we utilized a model in which lean and obese mice were initially infected with a sublethal dose of influenza A/PR/8/34 (H1N1, PR8). After 5 wk, mice were challenged with a lethal dose of heterologous pandemic A/Cal/04/09 (H1N1, pH1N1). Similar to results shown previously in lean, chow fed mice (21), we found that priming with PR8 effectively prevented mortality from pH1N1 infection in both lean and obese mice in the absence of cross-reactive neutralizing antibodies. However, obese mice exhibited a lower level of cross-reactive pH1N1 nucleoprotein (NP) antibodies 5 wk after the PR8 infection, and a lower proportion of obese mice generated pH1N1 HAI antibodies following the secondary challenge. Consequently, obese mice had greater lung viral titers, more lung pathology as well as an increased number of cytotoxic memory $CD8^+$ T cells in lung airways during the pH1N1 infection. Given the excessive inflammation, infiltration, lung damage and cytotoxic

$CD8^+$ T-cell responses in the lungs of obese mice during the lethal pH1N1 challenge, we investigated the impact of obesity on regulatory T cells (Tregs) as a potential mechanism for the inability to control the antiviral responses in the lung. Unexpectedly, obese mice had nearly twice as many Tregs in the lung airways during the heterologous secondary pH1N1 infection compared with lean mice. However, *ex vivo* analysis of Treg function revealed that Tregs isolated from obese mice were significantly less suppressive than those isolated from lean mice. Therefore, an excessive inflammatory response in the lungs, potentially due to a combination of elevated viral titers and impaired Treg function, may be a mechanism by which obesity enhances pH1N1 infection severity.

Materials and methods

Mice and diets

Weanling, male, C57BL/6J mice were obtained from The Jackson Laboratory (Bar Harbor, ME) and fed a low fat diet with 10% kcal fat (Research Diets D12450B) or high fat diet with 45% kcal fat (Research Diets D12451, New Brunswick, NJ). In addition to inducing weight gain, high fat diets are considered to be pro-inflammatory (41). Mice were maintained on the diets for 15–18 wk as described below. Mice were housed in isolation cubicles at the University of North Carolina Animal Facility (fully accredited by the American Association for Accreditation of Laboratory Animal Care). All experimental procedures involving mice were approved by the UNC Institutional Animal Care and Use Committee.

Influenza virus and infection in mice

Influenza A/Puerto Rico/8/34 (H1N1, PR8), obtained from American Type Culture Collection (Manassas, VA), was utilized for primary infections. Pandemic influenza A/California/04/09 (H1N1, pH1N1) was obtained from BEI resources (Manassas, VA) and was used for secondary infections. Both PR8 and pH1N1 were propagated in the allantoic cavities of 10–12-day-old embryonated chicken eggs. At 72 h post-infection, allantoic fluid from eggs was harvested and clarified by centrifugation at 5000 × rpm for 10 min at 4°C, aliquoted and stored at −80°C. The stock viral titers of PR8 and pH1N1 were determined by a modified 50% tissue culture infective dose ($TCID_{50}$) in Madin-Darby canine kidney cells using hemagglutination as an endpoint (42) and evaluated by the method of Reed and Muench (43). For influenza inoculations, mice were lightly anesthetized by isoflurane inhalation and inoculated via non-invasive oral aspiration (44, 45) with 0.05mL of viral inoculum diluted in PBS. For re-challenge studies, mice were maintained on the designated low fat or high fat diet for 15 wk and then infected with 11.4 $TCID_{50}$ PR8 for a primary infection. Mice were monitored and weighed daily for 14 days post-infection (dpi) following the primary PR8 infection. Five weeks after the primary PR8 infection, a similar period of time as performed by others (27, 30, 38, 46), mice were rechallenged with 5×10^3 $TCID_{50}$ pH1N1, a previously determined lethal dose (approximately 10 LD_{50}). Following the secondary pH1N1 infection, mice were weighed daily. For isolation of Treg cells from mouse splenocytes or harvesting of sera during the primary PR8 infection, mice were maintained on a high fat or low fat diet for 18 wk.

Quantitation of viral titers

Viral titers in lung tissue were determined by a modified $TCID_{50}$ using hemagglutination as an endpoint as previously described (47). Briefly, the lung tissue from lavaged mice was harvested and frozen in liquid nitrogen for subsequent processing. The supernatant from each homogenized lung was collected, serially diluted and added to 80% confluent Madin-Darby canine kidney cells in replicates of six in 96-well pates. $TCID_{50}$ was determined using the Reed and Muench method (43), and values were normalized to lung tissue weight (38).

Hemagglutination inhibition and microneutralization assays

Sera were collected from individual mice, at days 0 (five weeks after the primary PR8 infection, naïve to pH1N1), 5, 8 and 14 following the secondary pH1N1 challenge and hemagglutination inhibition (HAI) titers were determined. Briefly, sera were treated with receptor destroying enzyme (RDE; Denka Seiken, Tokyo, Japan) overnight, followed by inactivation at 56°C for 1 h, and a final dilution to 1:10 with PBS. RDE-treated sera were then incubated with either pH1N1, PR8 or influenza A/Victoria/361/2011 (negative control) for 15 min at room temperature (primary PR8 infection sera was incubated with PR8 alone). After a 1 h incubation at 4°C with either 0.5% turkey RBC (PR8, pH1N1) or 0.5% chicken RBC (PR8, A/Victoria/361/2011), HAI titer was determined by the reciprocal of the highest dilution of serum to completely inhibit hemagglutination. Positive and negative controls as well as back titrations of virus were included on each individual plate.

Microneutralization assays were performed on sera from PR8-infected mice at 35 dpi as previously described (48). Briefly, 100 $TCID_{50}$ of either PR8 or CA/09 were added to two-fold dilutions of RDE-treated sera, and serum-virus mixtures were incubated at 37°C, 5% CO_2 for 1 h. Following incubation, 3×10^5 MDCK cells were added to each well and plates were incubated overnight at 37°C, 5% CO_2. Plates where then fixed with 80% acetone, blocked for 2 hours at room temperature and an ELISA was performed using mouse anti-influenza A NP monoclonal antibody mixture (BEI Resources) followed by Peroxidase-conjugated goat anti-mouse IgG (Jackson Immunoresearch, West Grove, PA). ELISA plates were developed for 10 min using Substrate Reagent (R&D Systems, Minneapolis, MN), stopped using a 2N H_2SO_4 solution and absorbance of each well was read at 450nm. Wells were considered positive for microneutralization at an OD below or equal to 50% of the MDCK cells being infected.

Influenza nucleoprotein ELISA

Anti-nucleoprotein antibodies in the sera of lean and obese mice 35 days after the primary PR8 infection were measured by ELISA. Briefly, 8ug/mL of purified pH1N1 nucleoprotein (A/California//06/2009, Immune Technology Corp., New York, NY) was coated on ELISA plates (BD Falcon, San Jose, CA) overnight at 4°C in coating buffer. Influenza A/Cal/04/2009 NP was not commercially available, so purified NP from the A/Cal/06/2009 pandemic strain was used. Subsequently, ELISA plates were blocked with 1% BSA for 1h at 37°C, washed and then incubated with mouse sera (1:400 dilution) overnight. Following the overnight incubation, plates were washed and incubated with HRP-conjugated goat anti-mouse IgG (Invitrogen, Carlsbad, CA) antibody (1:2000 dilution) for 1h at 37°C. After washing, the assay was developed with the TMB Substrate Kit (Thermo Scientific, Rockford, IL) per manufacturer's instructions. Optical density was measured at 405nm, and the optical density of uninfected control sera was subtracted from the 35 dpi experimental samples.

Lung histopathology

At 5 dpi, the left lobe of the lung was harvested from lean and obese mice, inflated with 4% paraformaldehyde and maintained in 4% paraformaldehyde for 48 h, after which samples were transferred to 70% ethanol. Tissues were paraffin embedded, and three 5μm (separated by 100μm) sections (per lung sample) were processed for H&E staining by the UNC Animal Histopathology Core Facility. The extent of lung pathology was scored blindly according to relative degree of mononuclear infiltrate on a scale from 0 to 4: 0, no inflammation; 1, mild influx of inflammatory cells; 2, increased inflammation with ~25–50% of the total lung involved; 3, severe inflammation involving 50–75% of the lung; and 4, almost all lung tissue contains inflammatory infiltrate (38).

Bronchoalveolar lavage total protein and albumin measurements

To recover bronchoalveolar lavage (BAL) fluid, the trachea of killed mice were exposed and cannulated with a 22-guage angiocath, and the lungs were then lavaged with a series of 4 washes with unsupplemented HBSS, totaling 3.75mL (one 0.75mL and three 1mL washes). BAL fluid supernatant was collected from the initial 0.75mL lavage and was subsequently used for total protein, and albumin detection. The cells from the series of BAL washes for each mouse were combined for subsequent flow cytometry analysis. BAL fluid was harvested at 5, 8 and 14 days following the secondary pH1N1 infection. BAL supernatants from 5 and 8 dpi were diluted 1:10, and total protein was measured (BCA kit, Sigma Aldrich, St Louis, MO). BAL supernatants were diluted 15,000 fold prior to measuring albumin levels per manufacturer instructions of the Mouse Albumin ELISA Kit (Genway Biotech, Inc., San Diego, CA).

Quantitation of lung cytokine gene expression

Lung tissue samples were collected at day 0 (five weeks after the primary PR8 infection, naïve to pH1N1) and 5, 8, and 14 days following the secondary pH1N1 infection. Total RNA was isolated using the TRIzol method (Invitrogen), and reverse transcription was performed with use of the Superscript II First Strand Synthesis kit (Invitrogen) using oligo (dT) primers. Expression levels of cytokines and chemokines were quantified using qRT-PCR as previously described (42).

Flow cytometry

Splenocytes and cells from draining mediastinal lymph nodes (mLN) were isolated as previously described (38). For analysis of surface proteins of T-cell populations, single-cell suspensions were simultaneously incubated with Fc blocker (anti-CD16/CD32) and stained in PBS (with 1% FBS) with the following monoclonal antibodies: CD3 (APC/Cy7), CD62L (Brilliant Violet 421) and CD8 (PerCP) from BioLegend (San Diego, CA); CD4 (FITC, PE-Cy7), CD25 (PE-Cy7), CCR7 (APC), CD44 (PE-Cy7) and CD62L (E450) from eBioscience (San Diego, CA). MHC class I tetrameric complexes (PE) specific for the H-2D^b-restricted epitope of the nucleoprotein (NP, D^{b}NP$_{366\text{-}74}$; ASNENMETM) of PR8 were used to identify NP-specific T cells and the irrelevant LCMV tetramer D^{b}GP$_{33\text{-}41}$ (PE) was used as a negative control (NIH Tetramer Core Facility, Atlanta, GA). For intracellular cytokine and transcription factor staining, cells were fixed and permeabilized with the Foxp3/ Transcription Factor Staining Buffer Set (eBiosciences) per manufacturer's instructions. Subsequently, cells were stained with Foxp3 (APC, eBioscience) for identification of Tregs. For detection of the intracellular cytokines IFN-γ (APC, eBioscience) and granzyme B (GzB, FITC, eBioscience), 1–5×10^5 BAL cells were stimulated under the following conditions for 6 h in the presence of Golgi Plug (BD Biosciences, San Jose, CA) per manufacturer instructions: incubated with heat-inactivated pH1N1 (inactivated by a 1 h incubation at 56°C) at a multiplicity of infection (MOI) of 1×10^{-3}; incubated with heat-inactivated pH1N1 (MOI=2×10^{-3}) with antigen-presenting cells (splenocytes from lean mice depleted of nonadherent cells) pulsed with heat-inactivated pH1N1 (MOI=0.1) at a ratio of 1 APC:15 BAL cells; or 0.08μg/mL of Con A. Samples were analyzed on a CyAn ADP Analyzer flow cytometer (Beckman Coulter, Inc., Fullerton, CA) and cytometry data were analyzed with FlowJo software (TreeStar, Ashland, OR). T-cell populations were analyzed by a doublet exclusion gate for all cells followed by gating of CD3$^+$ T cells for further analysis of CD4$^+$ and CD8$^+$ T-cell populations.

Suppression Assay

Treg suppression assays were performed similar to De Rosa et al. (49). Tregs were isolated from pooled splenocytes of three naive lean or three naïve obese mice. CD4$^+$CD25$^+$ Tregs

and $CD4^+CD25^-$ T effector cells (Teff) were isolated using the Dynabeads FlowComp Mouse $CD4^+CD25^+$ Treg Cells kit (Invitrogen) and stimulated with Dynabeads mouse anti-CD3/28 (0.5 bead/Teff; 5×10^4 Teff per well). The Treg cells (≥95% $Foxp3^+$ by FACS analysis) and Teff cells (≤5% $Foxp3^+$) were cocultured at a ratio of 1:2 in round-bottom 96-well plates with complete RPMI medium. Only Teff cells from lean mice were used in the assay to eliminate concern of a discrepancy in obese mouse Teff cell proliferation. Cells were stimulated for 72 h, and cells were pulsed with [3^H]thymidine (PerkinElmer, Boston, MA) for the last 16 h of culture. Cells were harvested onto glass fiber filter paper (Brandel Inc., Gaithersburg, MD), and radioactivity was measured using a Wallac 1409 liquid scintillation counter (Wallac, Turku, Finland).

Statistical analysis

JMP Statistical Software (SAS Institute, Cary, NC) was used for all statistical analyses. Statistical significance for parametric data was evaluated using the two-tailed unpaired Student *t* test to compare dietary groups. For nonparametric data, the Wilcoxon signed rank test was used. Lastly, for the percentage of mice with HAI titers at each dpi, the 2-tailed Fisher's exact test was used. Differences between means were considered significantly different at $p<0.05$.

Results

Heterologous immune defenses prevent mortality from a lethal pH1N1 challenge in lean and obese mice

To investigate the impact of obesity on heterologous immunity to a lethal pH1N1 infection, we utilized a diet-induced obese mouse model. To induce obesity, weanling, male C57BL/6J mice were fed a high fat (45% kcal from fat) diet or a low fat (10% kcal from fat) control diet for 15 wk (Fig. 1A). The OpenSource Diets® are composed of purified constituents and are matched in every aspect except for fat and carbohydrate content. Mice fed a high fat diet rapidly gained more weight than control mice and after 15 wk on the diet weighed approximately 33% more (Fig. 1B). Mice were maintained on the respective high fat or low fat diet throughout the course of the experiment, including both primary and secondary infections.

To test if obese mice had compromised heterologous defenses, lean and obese mice were initially infected with a sublethal dose of PR8 virus after the 15 wk of dietary exposure (Fig. 1A). As expected, obese mice lost significantly more weight (5.10±0.40g) compared with lean mice (3.54±0.31g) following the primary PR8 infection, but when normalized to pre-infection body weight, there were no differences in percent weight loss between lean and obese mice (Fig. 1C). PR8 infected mice were maintained on their respective diets for 5 wk to allow the mice sufficient time to recover. After 5 wk, having regained weight equivalent to initial weight status prior to the PR8 infection (data not shown), mice were infected with a lethal dose of pH1N1 virus. One-hundred percent of naïve (unprimed) lean and obese mice rapidly succumbed to the lethal pH1N1 infection at 6 dpi (Fig. 1D). However, of the mice previously infected with PR8, 100% of lean mice and 95% of obese mice survived the pH1N1 challenge. Contrary to the initial primary infection, both lean and obese mice began to lose weight early at 2 dpi following the secondary pH1N1 infection, with obese mice nearly losing twice as much weight as lean mice over the course of the infection. However, once normalized to body weight, weight loss was not significantly different between the two groups (Fig. 1E).

Diet-induced obesity impairs primary and secondary influenza antibody responses

We assayed sera for HAI antibodies 5 wk following the primary PR8 infection in lean and obese mice to confirm that the pH1N1 virus was heterologously distinct in our hands. We did not detect HAI antibodies to pH1N1 in sera from lean or obese mice previously infected with PR8 (Fig. 2A). Further, microneutralization assays confirmed that the PR8 infection did not induce cross-neutralizing protection to pH1N1 virus (Fig. 2B). Similarly, Guo et al. did not detect cross-neutralizing antibodies to pH1N1 in sera from PR8-infected mice (21). Therefore, reflective of what happened in the human population during the pH1N1 outbreak, PR8 infected mice lacked pH1N1cross-reactive neutralizing antibodies.

As expected, 5 wk after PR8 infection, lean mice displayed elevated HAI and microneutralization titers to PR8 but not pH1N1 (Fig. 2A/B). Surprisingly, none of the obese mice had detectable HAI antibodies to PR8, and obese mice had nearly a 4-fold lower PR8 microneutralization titer. Although PR8 HAI antibodies are not critical modulators of secondary infection outcome in this model, the striking deficiency in PR8 HAI antibodies prompted us to measure PR8 antibody levels during the primary PR8 infection to determine if the reduced antibody levels at 35 dpi were a result of decreased antibody generation. At 7 dpi following the primary PR8 infection, obese mice had a lower mean PR8 HAI titer and a lower percentage of obese mice (p=0.06) exhibited detectable PR8 HAI antibodies (Fig. 2C/D). However, by 9 dpi and through 14 dpi, obese mice had similar levels of HAI antibodies compared with lean mice. Therefore, obese mice exhibited delayed antibody generation during the primary infection but were able to compensate and eventually exhibited similar levels to that of lean mice. However, by 35 dpi, obese mice did not have any detectable PR8 HAI antibodies (Fig. 2C/D), indicating that obesity also impairs antibody maintenance. Kim et al. demonstrated that obese mice have impaired responsiveness to influenza vaccination, but obesity-induced impairments in antibody responses following infection in mice have not previously been shown (40). Interestingly, we have similarly demonstrated that obese humans have an impaired ability to maintain long-term levels of influenza antibodies (39).

Because of the striking deficiency of PR8 HAI antibodies in the obese mice at 35 dpi, we also assessed pH1N1 HAI antibody levels following the secondary challenge. Previous studies in mice have demonstrated that a primary heterologous influenza infection can lead to an accelerated production of pH1N1 neutralizing antibodies during a secondary pH1N1 infection (25, 30), which could potentially impact infection outcome. We did not detect HAI antibodies at 5 dpi in lean or obese mice; however, 72.7% of lean mice had HAI antibodies at 8 dpi. By 14 dpi, 100% of lean mice had HAI antibodies (Fig. 3A/B). In contrast to lean mice, 41.7% of obese mice generated detectable serum HAI antibodies at 8 dpi, and only 50% of obese mice had pH1N1 HAI antibodies at 14 dpi (Fig. 3A/B). Therefore, obese mice displayed altered antibody responses during both primary and secondary infections. Although PR8 HAI antibodies offer negligible protection during the secondary infection, we measured PR8 HAI antibodies to determine if the impairments in antibody production during the secondary infection were specific to pH1N1 or a more global defect. The differences between lean and obese mice were striking, as 75% (day 5), 72.7% (day 8) and 83.3% (day 14) of lean mice had detectable levels of HAI antibodies to PR8 during the secondary pH1N1 infection compared with 8.3% (day 5), 16.7% (day 8) and 33.3% (day 14) of obese mice (Fig. 3C/D). As a negative control for all HAI titers from sera obtained during the secondary infection, influenza A/Victoria/361/2011 (H3N2) was assayed in addition to pH1N1 and PR8. Taken together, obese mice exhibited delayed or impaired antibody generation during primary and secondary influenza infections, respectively, and impaired antibody maintenance (35 days following the primary PR8 infection).

Although, PR8 antibodies do not neutralize pH1N1 virus infectivity (see Figure 2B), nucleoprotein (NP) specific antibodies generated during a heterologous primary influenza

infection or through vaccination have been shown to control virus replication during influenza infections (29, 50, 51). Therefore, we next assayed the level of anti-pH1N1 NP antibodies in lean and obese mice at 35 dpi. Interestingly, we detected that obese mice had a significantly lower level of serum anti-pH1N1 NP antibodies (Figure 3E). Because NP antibodies can regulate viral burden (29), we next measured lung viral titers in lean and obese mice to determine if lower anti-NP antibody levels potentially impacted influenza viral titers during the secondary pH1N1 infection. At 5 dpi, obese mice had greater than a 10-fold higher mean virus titer (p=0.05) in the lungs compared with lean mice (Fig. 3F). Although viral replication is controlled through several cell types and effector responses, it is plausible that reduced NP antibody levels resulted in greater viral burden in the lungs of obese mice.

Obese mice develop greater lung airway inflammation following a secondary heterologous pH1N1 infection

Given that obese mice exhibited elevated viral titers at 5 dpi, we next assessed how greater viral burden impacted lung inflammation and pathology. Enumeration of BAL cells following the secondary infection revealed that obese mice had nearly twice as many cells in the lung airways at 5 dpi (Fig. 4A). Conversely, in the draining mLN, lean mice had approximately twice as many immune cells as obese mice at 5 dpi (Fig. 4B). Despite the lack of differences in inflammatory cytokine expression (Table I), obese mice had elevated lung pathology scores (Fig. 4C) and a greater level BAL fluid protein at 5 dpi (Figure 4D). To determine if the elevated level of immune cell infiltration and inflammation in the lungs resulted in damage to the integrity of the respiratory epithelium in obese mice, we assayed albumin levels in the lung airways. Consistent with heightened infiltrate and pathology at 5 dpi, we detected greater levels of BAL albumin at 5 dpi in obese mice (Figure 4E).

Obese mice have a heightened memory CD8$^+$ T-cell response in the lung airways following a lethal secondary pH1N1 infection

The protective role of memory T cells during secondary heterologous influenza infections is well established (52, 53). Further, several recent investigations have demonstrated that exposure to seasonal influenza strains or vaccination can elicit memory T cells that are able to recognize viral epitopes of pH1N1, conferring cross-protection (15, 25). Both CD4$^+$ and CD8$^+$ memory T cells have been shown to be important in limiting disease severity in several models of pH1N1 rechallenge studies (21, 25, 27).

To determine if obesity influenced the distribution and activation of cross-reactive T cells, BAL cells from mice previously infected with PR8 5 wk earlier and then challenged with pH1N1 were stimulated with heat-inactivated pH1N1 virus, pH1N1-pulsed APCs or the polyclonal mitogen, Con A, at days 5, 8 and 14 following the secondary pH1N1 infection. Figure 5A demonstrates that all three methods of stimulation induced a robust IFN-γ response in cross-reactive CD4$^+$ T cells at 5 dpi. As expected, the addition of influenza-pulsed APCs in culture with BAL cells resulted in an elevated IFN-γ response compared with BAL cells incubated with heat-inactivated virus alone. Obesity did not impair IFN-γ or GzB production by memory CD4$^+$ T cells in response to the stimuli (Fig. 5B/C). There were no differences in CD4$^+$ T-cell IFN-γ median fluorescence intensity (MFI) or GzB MFI (data not shown).

Next, we investigated potential differences in CD4$^+$ effector memory T cells between lean and obese mice as we have previously demonstrated that obese mice have an impaired CD8$^+$ effector memory T-cell response (38). Effector memory T cells were distinguished by lack of expression of the cell adhesion molecule, CD62L, which is inherently absent or low on effector memory T cells (54). Because we detected differences in viral titers and lung

pathology at 5 dpi, we focused on effector memory T-cell populations specifically on this day. However, we did not detect any differences in IFN-γ or GzB production of $CD4^+CD62L^-$ effector memory T cells between lean and obese mice (Fig. 5D/E). This suggests, at least partially, that cross-reactive $CD4^+$ T-cell cytotoxic responses are intact in obese mice.

We also determined how obesity affected the cross-reactive $CD8^+$ T-cell response under the same conditions described for $CD4^+$ T cells. Approximately, 4–5% of $CD8^+$ T cells from lean and obese mice produced IFN-γ following stimulation with influenza-pulsed APCs at 5 dpi (Fig. 6A). After day 5, the magnitude of the $CD8^+$ T-cell response declined in both lean and obese mice (Fig. 6B/C). Interestingly, obese mice had a strikingly elevated number of $CD8^+$IFN-γ^+ and $CD8^+GzB^+$ T cells at 5 dpi (Fig. 6B/C). Further analysis of the $CD8^+$ memory T-cell population revealed that obese mice had an elevated number of $CD8^+CD62L^-$IFN-γ^+ T cells and a significantly greater number of $CD8^+CD62L^-GzB^+$ effector memory T cells at 5 dpi as well (Fig. 6D/E). There were no differences in CD8+ IFN-γ MFI or GzB MFI (data not shown).

We used whole virus in BAL cell stimulations, and thus we were assessing the total polyclonal response of the $CD4^+$ and $CD8^+$ memory T-cell pool. Since we detected significant differences in the number of GzB producing effector memory $CD8^+$ T cells in obese mice, we next examined GzB production by effector memory T cells specific for a specified viral epitope. As NP from PR8 shares 91% similarity with the pH1N1 NP (30), we used the influenza tetramer $D^bNP_{366\text{-}74}$, allowing for detection of T cells specific for the PR8 $NP_{366\text{-}74}$ epitope during the secondary pH1N1 infection. Figure 6F demonstrates that obese mice had a greater number of $NP_{336\text{-}74}$ specific T cells producing GzB following stimulation. Further, obese mice had a significantly greater number of $NP_{366\text{-}74}$ specific $CD8^+CD62L^-$ T cells, and a significantly greater proportion of these cells produced GzB (Fig. 6G). The elevated cross-reactive $CD8^+$ T-cell response could be attributed to the greater viral burden detected in the lungs of obese mice at 5 dpi. It is likely that greater viral load induced excessive recruitment of $CD8^+$ T cells to the lungs, and perhaps the elevated $CD8^+$ T-cell response was required to control the excess viral burden in the absence of proper antibody defenses.

Obese mice have a greater number of $CD4^+CD25^+Foxp3^+$ Tregs in the lung airways at 5 dpi

Numerous factors could contribute to the increased lung inflammation, lung infiltration, lung damage and memory $CD8^+$ T-cell responses in obese mice. Enhanced inflammatory responses in the lungs between 1–5 dpi or altered expression of lung trafficking molecules on immune cells could result in the observed differences in infiltration in the lung at 5 dpi. However, we did not detect any differences in the percentage of mLN $CD8^+$ T cells expressing the trafficking molecules CD44, CD62L and CCR7 at 5 dpi, nor did we find any differences in mLN or lung chemokine expression at 0 or 5 dpi (mLN data not shown).

We observed greater infiltration, lung damage and heightened $CD8^+$ T-cell responses in the lungs of obese mice, and Tregs have been shown to regulate all of these parameters in other respiratory infection models (55, 56). Further, obesity has been reported to result in a deficiency of anti-inflammatory Tregs in metabolic tissues such as white adipose (57) and the liver (58). We therefore proceeded to investigate this unique cell type in the secondary infection model as a potential mechanism for increased inflammation in the obese mice. Figure 7A represents the gating scheme used to distinguish Tregs and demonstrates the Treg distribution in the lung airways and mLN in lean and obese mice at 5 dpi. Although, $CD25^-Foxp3^+$ Tregs were present in the lung airways and mLN following the secondary infection, the majority of $Foxp3^+$ T cells were $CD25^+$ (Fig. 7A). BAL Treg number peaked at 5 dpi in obese mice and continually decreased in number, whereas lean mice had

consistent numbers of BAL Tregs from 5 to 8 dpi with a similarly low level of Tregs by 14 dpi (Fig. 7B). Interestingly, obese mice had more than twice as many BAL Tregs at 5 dpi and nearly half as many mLN Tregs (Fig. 7C) compared with lean mice. Consistent with two recent publications investigating Tregs during a primary influenza infection (59, 60), the mLN in lean and obese mice contained a greater number of Tregs than the BAL compartment following infection (Fig. 7C). There is little known regarding memory Tregs during influenza infection nor the distribution and function of Tregs during a secondary influenza infection. One would expect a greater presence of suppressive Treg cells to result in a dampening of the inflammatory and cytotoxic responses in the lungs of obese mice (61). However, we observed the opposite, and therefore investigated the possibility that obese mice have impaired Treg suppressive function.

Tregs isolated from obese mice are less suppressive than those from lean mice

To compare Treg activity from lean and obese mice, we used a well-established suppression assay (49). Tregs isolated from splenocytes were cocultured in the presence of $CD4^+CD25^-$ Teff cells isolated from lean mice. Tregs from lean and obese mice were only cocultured with Teff cells isolated from lean mice to eliminate any possibility of a discrepancy in Teff proliferation between lean and obese mice. Figure 8A demonstrates that isolated Treg populations were greater than 95% $Foxp3^+$ from both dietary groups, and less than 5% of Teff cells isolated from lean mice were $Foxp3^+$, confirming pure populations of isolated cells. Interestingly, after a 72 h anti-CD3/CD28 polyclonal stimulation, Tregs isolated from obese mice were found to be significantly less suppressive (Fig. 8B). After normalizing to lean Treg activity, Tregs isolated from obese mice were 41% less suppressive (Fig. 8C). Therefore, diet-induced obesity dramatically impaired Treg suppressive activity. There are a wide variety of mechanisms that could contribute to the impaired Treg function in obese mice. The level of Foxp3 expression in Treg cells is important for suppressive activity as experimental reduction in Foxp3 results in impaired Treg suppressive function (62, 63). Thus, we assayed Foxp3 protein expression levels in Tregs from splenocytes of lean and obese mice, but we did not detect differences in Foxp3 levels (Fig. 8D) suggesting that impairment in Treg function is due to a mechanism unrelated to Foxp3 expression.

Discussion

Globally, greater than 1.4 billion adults are overweight, and approximately 500 million of these individuals are obese (36). In 2009, obesity was reported to be an independent risk factor for hospitalization and death following pH1N1 influenza infection (32–34). Given the prevalence of obesity and the consistent threat of influenza epidemics and pandemics, understanding how excess adiposity affects the immune response to influenza infection is important in potentially developing therapies to limit morbidity and mortality in this at-risk population.

During the 2009 pandemic, a majority of individuals (nonelderly) lacked pre-existing neutralizing antibody protection to pH1N1 (10, 12–15). Therefore, a number of investigations have focused on the protectiveness of heterologous immunity to pH1N1 infection, conferred from previous exposure to circulating influenza strains or vaccines (19, 27, 28). Human studies and mouse models have demonstrated that cross-reactive T cells and cross-reactive non-neutralizing antibody defenses can limit viral load and protect from a lethal heterologous influenza infection (10, 19, 21, 30). Additionally, prior heterologous infection can accelerate pH1N1 antibody generation during a secondary pH1N1 infection, thus providing an additional mechanism by which heterologous immunity can limit pH1N1 infection severity (25, 30). However, obese humans and mice have been shown to have impaired memory T-cell and humoral responses following vaccination or infection (38–40,

64). Thus, we developed a mouse model to investigate if obesity results in enhanced pH1N1 infection severity due to impairments in heterologous immune defenses.

In this study, obesity did not impair the overall ability of heterologous immunity to prevent mortality from pH1N1 infection as 95% of PR8 primed obese mice survived the lethal secondary heterologous infection, whereas none of the naïve, obese mice survived the pH1N1 infection. However, heterologous cellular and humoral responses were significantly altered by obesity, and obese mice displayed greater lung damage during the secondary pH1N1 infection. Obese mice exhibited a significant delay or impairment in antibody generation during both primary and secondary influenza infections. Further obese mice displayed significantly lower levels of cross-reactive anti-pH1N1 NP antibodies following the primary PR8 infection. Subsequent investigation of viral titers confirmed that obese mice had a greater lung viral titer at 5 dpi, perhaps due to reduced levels of cross-reactive anti-NP antibodies. Consistent with greater viral load, obese mice had an elevated number of infiltrating cells into the lung airways, heightened lung pathology, and greater BAL total protein and albumin levels. Analysis of cross-reactive T-cell responses demonstrated that obesity led to a heightened $CD8^+$ T-cell response in the lung airways, but obesity did not impact cross-reactive $CD4^+$ T-cell distribution during the secondary infection. These data point towards a model in which reduced levels of anti-NP antibodies resulted in greater lung viral burden, which subsequently induced greater immune cell infiltration, lung damage and heightened $CD8^+$ T-cell responses in obese mice. Lastly, we investigated the impact of obesity on Treg distribution during the secondary infection model. We found that obese mice had a greater number of BAL Tregs at 5 dpi, but *ex vivo* analysis revealed Tregs isolated from obese mice were significantly less functional than Tregs from lean mice. Therefore, perhaps obese individuals experienced greater pH1N1 infection severity due to a combination of impaired pH1N1 heterologous antibody defenses and excessive antiviral immune responses in the lungs, which could not be controlled properly due to dysfunctional Tregs.

Despite a lack of neutralizing antibody protection, antibody defenses may still impart protection to a lethal pH1N1 infection in our model. A protective role for cross-reactive non-neutralizing antibodies during influenza infection has been well established (29, 30, 50, 51). LaMere et al. demonstrated that intact antibody defenses (i.e. somatic hypermutation and class-switch recombination) were required for proper heterologous immunity in the classical X31 prime, PR8 challenge, heterologous infection model (29). Further, influenza NP vaccination or passive transfer of NP immune serum can limit viral replication in the lungs of PR8 infected mice (29). Therefore, non-neutralizing antibodies can impart antiviral activity, although the exact mechanisms by which anti-NP antibodies function remain unclear (29). Interestingly, NP was detected in the 2008/09 trivalent inactivated vaccine, and some individuals demonstrated increased levels of anti-NP antibodies following vaccination (51). Therefore, non-neutralizing NP antibody protection is clinically relevant as well. The non-neutralizing influenza antibody repertoire can also include antibodies targeting other internal viral proteins such as the matrix protein (M1) and nonstructural protein 1 (NS1) (29, 30). However, the protective role of antibodies specific to these proteins is less established and likely less protective compared with anti-NP antibodies (29, 30).

Another mechanism by which heterologous immunity may protect against pH1N1 is through the acceleration of homologous pH1N1 antibodies produced during a secondary pH1N1 challenge. A primary heterologous infection followed by a pH1N1 challenge has been shown to result in significantly enhanced production of pH1N1 neutralizing antibodies (25), split pH1N1 antibodies and anti-NP antibodies compared with naïve mice infected with pH1N1 (30). It is likely that cross-reactive $CD4^+$ T cells facilitate this accelerated homologous pH1N1 antibody production (25). We did not detect pH1N1 HAI antibodies at

the early time-point of 5 dpi, however, we found that a significantly lower proportion of obese mice exhibited detectable pH1N1 HAI antibodies 14 days after the secondary challenge. Therefore, it is unlikely that this aspect of heterologous immunity contributed to the observed outcomes in lean and obese mice. Of particular note, we found that obese mice displayed a delayed production and impaired maintenance of PR8 antibodies following the primary, sublethal PR8 infection. Further, obese mice had significantly lower mean PR8 HAI titers during the secondary infection, and a lower proportion of obese mice had detectable PR8 HAI antibodies at all of the time points assayed. Although PR8 HAI antibodies did not mediate protection in this model *per se*, the dramatic impact of obesity on influenza antibody responses has clear public health implications. Kim et al. demonstrated that obesity impairs the antibody response to pH1N1 vaccination in mice (40), but it has not been reported that obesity alters antibody responses during the context of an infection.

Excessive antiviral and inflammatory immune responses in the lung, contributing to severe immunopathology, are known to be one of the primary causes of influenza-related morbidity and mortality (65, 66). Further, fatal pH1N1 infection is associated with enhanced inflammation with high numbers of $CD8^+GzB^+$ cytotoxic T cells and excess local production of IFN-γ in the lung (66). We similarly detected greater inflammation, lung pathology and a greater number of $CD8^+GzB^+$ cytotoxic T cells in the lungs of obese mice infected with pH1N1. Although, only mild symptoms were experienced by a majority of individuals infected, severe immunopathology may partly explain why certain at-risk groups, such as obese humans, experienced a worse outcome to pH1N1 infection.

Obesity is characterized by a state of chronic inflammation, likely due, in part, to the simultaneous deficiency of Tregs in metabolic tissues (57). Because obesity negatively impacts Treg distribution, we hypothesized that obese mice would have fewer Tregs in their lungs, offering a potential explanation for the greater lung infiltration, inflammation, pathology, damage and the heightened memory $CD8^+$ T-cell responses detected in the lung airways at 5 dpi. Tregs have been shown to regulate all of these parameters in other respiratory infection models (55, 56, 67). Contrary to our expectations, we found that obese mice had nearly twice as many Tregs in the lung airways at 5 dpi compared with lean mice. Subsequent investigation of Treg function revealed that Tregs isolated from obese mice were 41% less suppressive than those isolated from lean mice. Therefore, impaired Treg function may have contributed to the excessive antiviral responses observed in the lungs of obese mice at 5 dpi. Although, we did not show impaired Treg suppressive function *in vivo* during the infection, the suppression assay suggests that *in vivo* function may be impaired as well.

Betts et al. demonstrated that a primary influenza infection results in a robust, antigen-specific Treg response, and influenza infection-induced Tregs were able to suppress antigen-specific $CD4^+$ and $CD8^+$ T-cell proliferation and cytokine production (60). Further, a recent study by Brincks et al. reported that during secondary influenza infections, antigen-specific memory Tregs exhibit accelerated accumulation in the lungs and mLN compared with primary infection responses and control memory $CD8^+$ T-cell proliferation in a MHC class II dependent antigen-specific manner (68). Interestingly, depletion of memory Tregs resulted in heightened $CD8^+$ T-cell responses, pulmonary inflammation and lung cytokine expression during a secondary influenza infection (68). It is possible that obesity-induced alterations in memory Treg responses could have contributed to the aberrant inflammatory responses observed in obese mice during the secondary pH1N1 infection.

We utilized a mouse model of diet-induced obesity and heterologous influenza infection in attempt to mirror clinical and epidemiological evidence. We found lower levels of non-neutralizing influenza NP antibodies, heightened cross-reactive $CD8^+$ T-cell responses,

greater viral titers and lung pathology, and impaired Treg function in obese mice. We propose that impaired antibody protection resulted in greater viral burden, which subsequently drove heightened inflammatory responses that were not properly controlled by dysfunctional Tregs. This study and numerous others have demonstrated obesity negatively impacts the immune response to influenza infection (38, 40, 42, 64, 69–71). Yet, the exact cellular and molecular mechanisms by which excess adiposity contributes to altered antiviral defenses remain unclear (37). It is possible that one global defect in all immune cells can explain impaired functionality in the obese, but it is more likely that a complex combination of altered signaling pathways and responses ultimately impairs immunity and results in greater influenza susceptibility (37).

Acknowledgments

We thank the National Institutes of Health Tetramer Facility and the University of North Carolina Flow Cytometry Core[3].

Abbreviations used in this paper

BAL	bronchoalveolar lavage
dpi	days post-infection
GzB	granzyme B
M1	influenza matrix protein
HAI	hemagglutination inhibition
MDCK	Madin-Darby canine kidney cells
MFI	median fluorescence intensity
MOI	multiplicity of infection
mLN	mediastinal lymph nodes
NP	influenza nucleoprotein
RDE	receptor destroying enzyme
pH1N1	pandemic H1N1 2009 influenza A virus, A/California/04/09
$TCID_{50}$	50% tissue culture infective dose
Teff	effector T-cell
Treg	regulatory T-cell
PR8	influenza A/Puerto Rico/8/34

References

1. Otte A, Sauter M, Alleva L, Baumgarte S, Klingel K, Gabriel G. Differential Host Determinants Contribute to the Pathogenesis of 2009 Pandemic H1N1 and Human H5N1 Influenza A Viruses in Experimental Mouse Models. Am J Pathol. 2011; 179:230–239. [PubMed: 21703405]
2. Itoh Y, Shinya K, Kiso M, Watanabe T, Sakoda Y, Hatta M, Muramoto Y, Tamura D, Sakai-Tagawa Y, Noda T. In vitro and in vivo characterization of new swine-origin H1N1 influenza viruses. Nature. 2009; 460:1021–1025. [PubMed: 19672242]

[3]The UNC Flow Cytometry Core Facility is supported in part by an NCI Center Core Support Grant (P30CA06086) to the UNC Lineberger Comprehensive Cancer Center.

3. Maines TR, Jayaraman A, Belser JA, Wadford DA, Pappas C, Zeng H, Gustin KM, Pearce MB, Viswanathan K, Shriver ZH. Transmission and pathogenesis of swine-origin 2009 A (H1N1) influenza viruses in ferrets and mice. Science. 2009; 325:484–487. [PubMed: 19574347]
4. Munster VJ, De Wit E, van den Brand JMA, Herfst S, Schrauwen EJA, Bestebroer TM, Van De Vijver D, Boucher CA, Koopmans M, Rimmelzwaan GF. Pathogenesis and transmission of swine-origin 2009 A (H1N1) influenza virus in ferrets. Science. 2009; 325:481–483. [PubMed: 19574348]
5. Presanis AM, De Angelis D, Hagy A, Reed C, Riley S, Cooper BS, Finelli L, Biedrzycki P, Lipsitch M. The severity of pandemic H1N1 influenza in the United States, from April to July 2009: a Bayesian analysis. PLoS Med. 2009; 6:e1000207. [PubMed: 19997612]
6. Kelly HA. A pandemic response to a disease of predominantly seasonal intensity. Med J Aust. 2010; 192:81–83. [PubMed: 20078407]
7. Update: novel influenza A (H1N1) virus infection-Mexico, March-May 2009. Morb Mortal Weekly Rep. 2009; 58:585–589.
8. Girard MP, Tam JS, Assossou OM, Kieny MP. The 2009 A (H1N1) influenza virus pandemic: A review. Vaccine. 2010; 28:4895–4902. [PubMed: 20553769]
9. Writing Committe of the WHO Consultation. Clinical Aspects of Pandemic 2009 Influenza A (H1N1) Virus Infection. N Engl J Med. 2010; 362:1708–1719. [PubMed: 20445182]
10. Hancock K, Veguilla V, Lu X, Zhong W, Butler EN, Sun H, Liu F, Dong L, DeVos JR, Gargiullo PM. Cross-reactive antibody responses to the 2009 pandemic H1N1 influenza virus. N Engl J Med. 2009; 361:1945–1952. [PubMed: 19745214]
11. Ikonen N, Strengell M, Kinnunen L, Osterlund P, Pirhonen J, Broman M, Davidkin I, Ziegler T, Julkunen I. High frequency of cross-reacting antibodies against 2009 pandemic influenza A (H1N1) virus among the elderly in Finland. Euro Surveill. 2010; 15:19478. [PubMed: 20144443]
12. Serum cross-reactive antibody response to a novel influenza A (H1N1) virus after vaccination with seasonal influenza vaccine. Morb Mortal Weekly Rep. 2009; 58:521–524.
13. Lee VJ, Tay JK, Chen MIC, Phoon M, Xie M, Wu Y, Lee CXX, Yap J, Sakharkar K, Sakharkar M. Inactivated trivalent seasonal influenza vaccine induces limited cross-reactive neutralizing antibody responses against 2009 pandemic and 1934 PR8 H1N1 strains. Vaccine. 2010; 28:6852–6857. [PubMed: 20723626]
14. Iorio A, Camilloni B, Lepri E, Neri M, Basileo M, Azzi A. Induction of Cross-Reactive Antibodies to 2009 Pandemic H1N1 Influenza Virus (pH1N1) After Seasonal Vaccination (Winters 2003/04 and 2007/08). Procedia Vaccinol. 2011; 4:50–58.
15. Iorio AM, Bistoni O, Galdiero M, Lepri E, Camilloni B, Russano AM, Neri M, Basileo M, Spinozzi F. Influenza viruses and cross-reactivity in healthy adults: Humoral and cellular immunity induced by seasonal 2007/2008 influenza vaccination against vaccine antigens and 2009 A (H1N1) pandemic influenza virus. Vaccine. 2012; 30:1617–1623. [PubMed: 22245606]
16. Valkenburg SA, Rutigliano JA, Ellebedy AH, Doherty PC, Thomas PG, Kedzierska K. Immunity to seasonal and pandemic influenza A viruses. Microb Infect. 2011; 13:489–501.
17. Thomas PG, Keating R, Hulse-Post DJ, Doherty PC. Cell-mediated protection in influenza infection. Emerg Infect Dis. 2006; 12:48–54. [PubMed: 16494717]
18. Ge X, Tan V, Bollyky PL, Standifer NE, James EA, Kwok WW. Assessment of seasonal influenza A virus-specific CD4 T-cell responses to 2009 pandemic H1N1 swine-origin influenza A virus. J Virol. 2010; 84:3312–3319. [PubMed: 20071564]
19. Tu W, Mao H, Zheng J, Liu Y, Chiu SS, Qin G, Chan PL, Lam KT, Guan J, Zhang L, Guan Y, Yuen K, Peiris J, Lau Y. Cytotoxic T lymphocytes established by seasonal human influenza cross-react against 2009 pandemic H1N1 influenza virus. J Virol. 2010; 84:6527–6535. [PubMed: 20410263]
20. Subbramanian RA, Basha S, Shata MT, Brady RC, Bernstein DI. Pandemic and seasonal H1N1 influenza hemagglutinin-specific T cell responses elicited by seasonal influenza vaccination. Vaccine. 2010; 28:8258–8267. [PubMed: 21050903]
21. Guo H, Santiago F, Lambert K, Takimoto T, Topham DJ. T cell-mediated protection against lethal 2009 pandemic H1N1 influenza virus infection in a mouse model. J Virol. 2011; 85:448–455. [PubMed: 20980523]

22. Greenbaum JA, Kotturi MF, Kim Y, Oseroff C, Vaughan K, Salimi N, Vita R, Ponomarenko J, Scheuermann RH, Sette A. Pre-existing immunity against swine-origin H1N1 influenza viruses in the general human population. Proc Natl Acad Sci U S A. 2009; 106:20365–20370. [PubMed: 19918065]
23. Xing Z, Cardona CJ. Preexisting immunity to pandemic (H1N1) 2009. Emerg Infect Dis. 2009; 15:1847–1549. [PubMed: 19891882]
24. Skountzou I, Koutsonanos DG, Kim JH, Powers R, Satyabhama L, Masseoud F, Weldon WC, del Pilar Martin M, Mittler RS, Compans R, Jacob J. Immunity to pre-1950 H1N1 influenza viruses confers cross-protection against the pandemic swine-origin 2009 A (H1N1) influenza virus. J Immunol. 2010; 185:1642–1649. [PubMed: 20585035]
25. Alam S, Sant AJ. Infection with Seasonal Influenza Virus Elicits CD4 T Cells Specific for Genetically Conserved Epitopes That Can Be Rapidly Mobilized for Protective Immunity to Pandemic H1N1 Influenza Virus. J Virol. 2011; 85:13310–13321. [PubMed: 21976658]
26. Hillaire MLB, van Trierum SE, Kreijtz JHCM, Bodewes R, Geelhoed-Mieras MM, Nieuwkoop NJ, Fouchier RAM, Kuiken T, Osterhaus ADME, Rimmelzwaan GF. Cross-protective immunity to influenza pH1N1 2009 viruses induced by seasonal A (H3N2) virus is mediated by virus-specific T cells. J Gen Virol. 2011; 92:2339–2349. [PubMed: 21653752]
27. Sun K, Ye J, Perez DR, Metzger DW. Seasonal FluMist vaccination induces cross-reactive T cell immunity against H1N1 (2009) influenza and secondary bacterial infections. J Immunol. 2011; 186:987–993. [PubMed: 21160043]
28. Couch RB, Atmar RL, Franco LM, Quarles JM, Niño D, Wells JM, Arden N, Cheung S, Belmont JW. Prior infections with seasonal influenza A/H1N1 virus reduced the illness severity and epidemic intensity of pandemic H1N1 influenza in healthy adults. Clin Infect Dis. 2012; 54:311–317. [PubMed: 22075792]
29. LaMere MW, Lam HT, Moquin A, Haynes L, Lund FE, Randall TD, Kaminski DA. Contributions of antinucleoprotein IgG to heterosubtypic immunity against influenza virus. J Immunol. 2011; 186:4331–4339. [PubMed: 21357542]
30. Fang Y, Banner D, Kelvin AA, Huang SSH, Paige CJ, Corfe SA, Kane KP, Bleackley RC, Rowe T, Leon AJ. Seasonal H1N1 Influenza Virus Infection Induces Cross-Protective Pandemic H1N1 Virus Immunity through a CD8-Independent, B Cell-Dependent Mechanism. J Virol. 2012; 86:2229–2238. [PubMed: 22130540]
31. Intensive-care patients with severe novel influenza A (H1N1) virus infection-Michigan, June 2009. Morb Mortal Wkly Rep. 2009; 58:749–752.
32. Louie JK, Acosta M, Samuel MC, Schechter R, Vugia DJ, Harriman K, Matyas BT. A novel risk factor for a novel virus: obesity and 2009 pandemic influenza A (H1N1). Clin Infect Dis. 2011; 52:301–312. [PubMed: 21208911]
33. Morgan OW, Bramley A, Fowlkes A, Freedman DS, Taylor TH, Gargiullo P, Belay B, Jain S, Cox C, Kamimoto L. Morbid obesity as a risk factor for hospitalization and death due to 2009 pandemic influenza A (H1N1) disease. PLoS One. 2010; 5:e9694. [PubMed: 20300571]
34. Jain S, Kamimoto L, Bramley AM, Schmitz AM, Benoit SR, Louie J, Sugerman DE, Druckenmiller JK, Ritger KA, Chugh R. Hospitalized patients with 2009 H1N1 influenza in the United States, April–June 2009. N Engl J Med. 2009; 361:1935–1944. [PubMed: 19815859]
35. Van Kerkhove MD, Vandemaele KAH, Shinde V, Jaramillo-Gutierrez G, Koukounari A, Donnelly CA, Carlino LO, Owen R, Paterson B, Pelletier L, Vachon J, Gonzalez C, Hongjie Y, Zijian F, Chuang SK, Au A, Buda S, Krause G, Haas W, Bonmarin I, Taniguichi K, Nakajima K, Shobayashi T, Takayama Y, Sunagawa T, Heraud JM, Orelle A, Palacios E, van der Sande MA, Wielders CC, Hunt D, Cutter J, Lee VJ, Thomas J, Santa-Olalla P, Sierra-Moros MJ, Hanshaoworakul W, Ungchusak K, Pebody R, Jain S, Mounts AW. and WHO Working Group for Risk Factors for Severe H1N1pdm Infection. Risk factors for severe outcomes following 2009 influenza A (H1N1) infection: a global pooled analysis. PLoS Med. 2011; 8:e1001053. [PubMed: 21750667]
36. World Health Organization. WHO Factsheet 311: Obesity and Overweight. May. 2012 [cited 2 August, 2012]http://www.who.int/mediacentre/factsheets/fs311/en/index.html
37. Milner JJ, Beck MA. The impact of obesity on the immune response to infection. Proc Nutr Soc. 2012; 71:298–306. [PubMed: 22414338]

38. Karlsson EA, Sheridan PA, Beck MA. Diet-Induced Obesity Impairs the T Cell Memory Response to Influenza Virus Infection. J Immunol. 2010; 184:3127–3133. [PubMed: 20173021]
39. Sheridan P, Paich H, Handy J, Karlsson E, Hudgens M, Sammon A, Holland L, Weir S, Noah T, Beck M. Obesity is associated with impaired immune response to influenza vaccination in humans. Int J Obes. 2011 Epub ahead of print.
40. Kim YH, Kim JK, Kim DJ, Nam JH, Shim SM, Choi YK, Lee CH, Poo H. Diet-induced obesity dramatically reduces the efficacy of a 2009 pandemic H1N1 vaccine in a mouse model. J Infect Dis. 2012; 205:244–251. [PubMed: 22147801]
41. Gianazza E, Sensi C, Eberini I, Gilardi F, Giudici M, Crestani M. Inflammatory serum proteome pattern in mice fed a high-fat diet. Amino Acids. 2012
42. Smith AG, Sheridan PA, Harp JB, Beck MA. Diet-induced obese mice have increased mortality and altered immune responses when infected with influenza virus. J Nutr. 2007; 137:1236–1243. [PubMed: 17449587]
43. Reed LJ, Muench H. A simple method of estimating fifty per cent endpoints. Am J Epidemiol. 1938; 27:493–497.
44. Wortham BW, Eppert BL, Motz GT, Flury JL, Orozco-Levi M, Hoebe K, Panos RJ, Maxfield M, Glasser SW, Senft AP, Raulet DH, Borchers MT. NKG2D Mediates NK Cell Hyperresponsiveness and Influenza-Induced Pathologies in a Mouse Model of Chronic Obstructive Pulmonary Disease. J Immunol. 2012; 188:4468–4475. [PubMed: 22467655]
45. Glasser SW, Witt TL, Senft AP, Baatz JE, Folger D, Maxfield MD, Akinbi HT, Newton DA, Prows DR, Korfhagen TR. Surfactant protein C-deficient mice are susceptible to respiratory syncytial virus infection. Am J Phsiol Lung Cell Mol Physiol. 2009; 297:L64–L72.
46. Snell LM, McPherson AJ, Lin GHY, Sakaguchi S, Pandolfi PP, Riccardi C, Watts TH. CD8 T cell-intrinsic GITR is required for T cell clonal expansion and mouse survival following severe influenza infection. J Immunol. 2010; 185:7223–7234. [PubMed: 21076066]
47. Farag-Mahmod FI, Wyde PR, Rosborough JP, Six HR. Immunogenicity and efficacy of orally administered inactivated influenza virus vaccine in mice. Vaccine. 1988; 6:262–268. [PubMed: 3420975]
48. World Health Organization. Serological diagnosis of influenza by microneutralization assay. Dec 6. 2010 [cited 18 Dec 2012]http://www.who.int/influenza/gisrs_laboratory/2010_12_06_serological_diagnosis_of_influenza_by_microneutralization_assay.pdf
49. De Rosa V, Procaccini C, Calì G, Pirozzi G, Fontana S, Zappacosta S, La Cava A, Matarese G. A key role of leptin in the control of regulatory T cell proliferation. Immunity. 2007; 26:241–255. [PubMed: 17307705]
50. Carragher DM, Kaminski DA, Moquin A, Hartson L, Randall TD. A novel role for non-neutralizing antibodies against nucleoprotein in facilitating resistance to influenza virus. J Immunol. 2008; 181:4168–4176. [PubMed: 18768874]
51. LaMere MW, Moquin A, Lee FE, Misra RS, Blair PJ, Haynes L, Randall TD, Lund FE, Kaminski DA. Regulation of antinucleoprotein IgG by systemic vaccination and its effect on influenza virus clearance. J Virol. 2011; 85:5027–5035. [PubMed: 21367900]
52. Flynn KJ, Belz GT, Altman JD, Ahmed R, Woodland DL, Doherty PC. Virus-specific CD8 T cells in primary and secondary influenza pneumonia. Immunity. 1998; 8:683–691. [PubMed: 9655482]
53. Effros RB, Doherty PC, Gerhard W, Bennink J. Generation of both cross-reactive and virus-specific T-cell populations after immunization with serologically distinct influenza A viruses. J Exp Med. 1977; 145:557–568. [PubMed: 233901]
54. Sallusto F, Lenig D, Förster R, Lipp M, Lanzavecchia A. Two subsets of memory T lymphocytes with distinct homing potentials and effector functions. Nature. 1999; 401:708–712. [PubMed: 10537110]
55. Loebbermann J, Thornton H, Durant L, Sparwasser T, Webster KE, Sprent J, Culley FJ, Johansson C, Openshaw PJ. Regulatory T cells expressing granzyme B play a critical role in controlling lung inflammation during acute viral infection. Mucosal Immunol. 2012; 5:161–172. [PubMed: 22236998]

56. Fulton RB, Meyerholz DK, Varga SM. Foxp3+ CD4 Regulatory T Cells Limit Pulmonary Immunopathology by Modulating the CD8 T Cell Response during Respiratory Syncytial Virus Infection. J Immunol. 2010; 185:2382–2392. [PubMed: 20639494]
57. Deiuliis J, Shah Z, Shah N, Needleman B, Mikami D, Narula V, Perry K, Hazey J, Kampfrath T, Kollengode M. Visceral adipose inflammation in obesity is associated with critical alterations in t regulatory cell numbers. PloS One. 2011; 6:e16376. [PubMed: 21298111]
58. Ma X, Hua J, Mohamood AR, Hamad ARA, Ravi R, Li Z. A high-fat diet and regulatory T cells influence susceptibility to endotoxin-induced liver injury. Hepatology. 2007; 46:1519–1529. [PubMed: 17661402]
59. Betts RJ, Ho AWS, Kemeny DM. Partial Depletion of Natural CD4 CD25 Regulatory T Cells with Anti-CD25 Antibody Does Not Alter the Course of Acute Influenza A Virus Infection. PloS One. 2011; 6:e27849. [PubMed: 22125630]
60. Betts RJ, Prabhu N, Ho AWS, Lew FC, Hutchinson PE, Rotzschke O, Macary PA, Kemeny DM. Influenza A Virus Infection Results in a Robust, Antigen-Responsive, and Widely Disseminated Foxp3 Regulatory T Cell Response. J Virol. 2012; 86:2817–2825. [PubMed: 22205730]
61. Sehrawat S, Rouse BT. Tregs and infections: on the potential value of modifying their function. J Leukoc Biol. 2011; 90:1079–1087. [PubMed: 21914856]
62. Wan YY, Flavell RA. Regulatory T-cell functions are subverted and converted owing to attenuated Foxp3 expression. Nature. 2007; 445:766–770. [PubMed: 17220876]
63. Josefowicz SZ, Lu LF, Rudensky AY. Regulatory T cells: mechanisms of differentiation and function. Annu Rev Immunol. 2012; 30:531–564. [PubMed: 22224781]
64. Karlsson EA, Sheridan PA, Beck MA. Diet-induced obesity in mice reduces the maintenance of influenza-specific CD8 memory T cells. J Nutr. 2010; 140:1691–1697. [PubMed: 20592105]
65. Damjanovic D, Small C, Jeyananthan M, McCormick S, Xing Z. Immunopathology in influenza virus infection: Uncoupling the friend from foe. Clin Immunol. 2012; 144:57–69. [PubMed: 22673491]
66. Mauad T, Hajjar LA, Callegari GD, da Silva LFF, Schout D, Galas FRBG, Alves VAF, Malheiros DMAC, Auler JOC, Ferreira AF, Borsato MRL, Bezerra SM, Gutierrez PS, Caldini ETEG, Pasqualucci CA, Dolhnikoff M, Saldiva PHN. Lung Pathology in Fatal Novel Human Influenza A (H1N1) Infection. Am J Respir Crit Care Med. 2010; 181:72–79. [PubMed: 19875682]
67. Lee DCP, Harker JAE, Tregoning JS, Atabani SF, Johansson C, Schwarze J, Openshaw PJM. CD25+ Natural Regulatory T Cells Are Critical in Limiting Innate and Adaptive Immunity and Resolving Disease following Respiratory Syncytial Virus Infection. J Virol. Sep 1.2010 84:8790–8798. [PubMed: 20573822]
68. Brincks EL, Roberts AD, Cookenham T, Sell S, Kohlmeier JE, Blackman MA, Woodland DL. Antigen-Specific Memory Regulatory CD4 Foxp3 T Cells Control Memory Responses to Influenza Virus Infection. J Immunol. 2013; 190:3438–3446. [PubMed: 23467933]
69. O'Brien KB, Vogel P, Duan S, Govorkova EA, Webby RJ, McCullers JA, Schultz-Cherry S. Impaired Wound Healing Predisposes Obese Mice to Severe Influenza Virus Infection. J Infect Dis. 2012; 205:252–261. [PubMed: 22147799]
70. Easterbrook JD, Dunfee RL, Schwartzman LM, Jagger BW, Sandouk A, Kash JC, Memoli MJ, Taubenberger JK. Obese mice have increased morbidity and mortality compared to non-obese mice during infection with the 2009 pandemic H1N1 influenza virus. Influenza Other Respi Viruses. 2011; 5:418–425. [PubMed: 21668672]
71. Zhang AJ, To KK, Li C, Lau CC, Poon VK, Chan CC, Zheng B, Hung IF, Lam KS, Xu A. Leptin mediates the pathogenesis of severe 2009 pandemic influenza A (H1N1) infection associated with cytokine dysregulation in mice with diet-induced obesity. J Infect Dis. 2013; 207:1270–1280. [PubMed: 23325916]

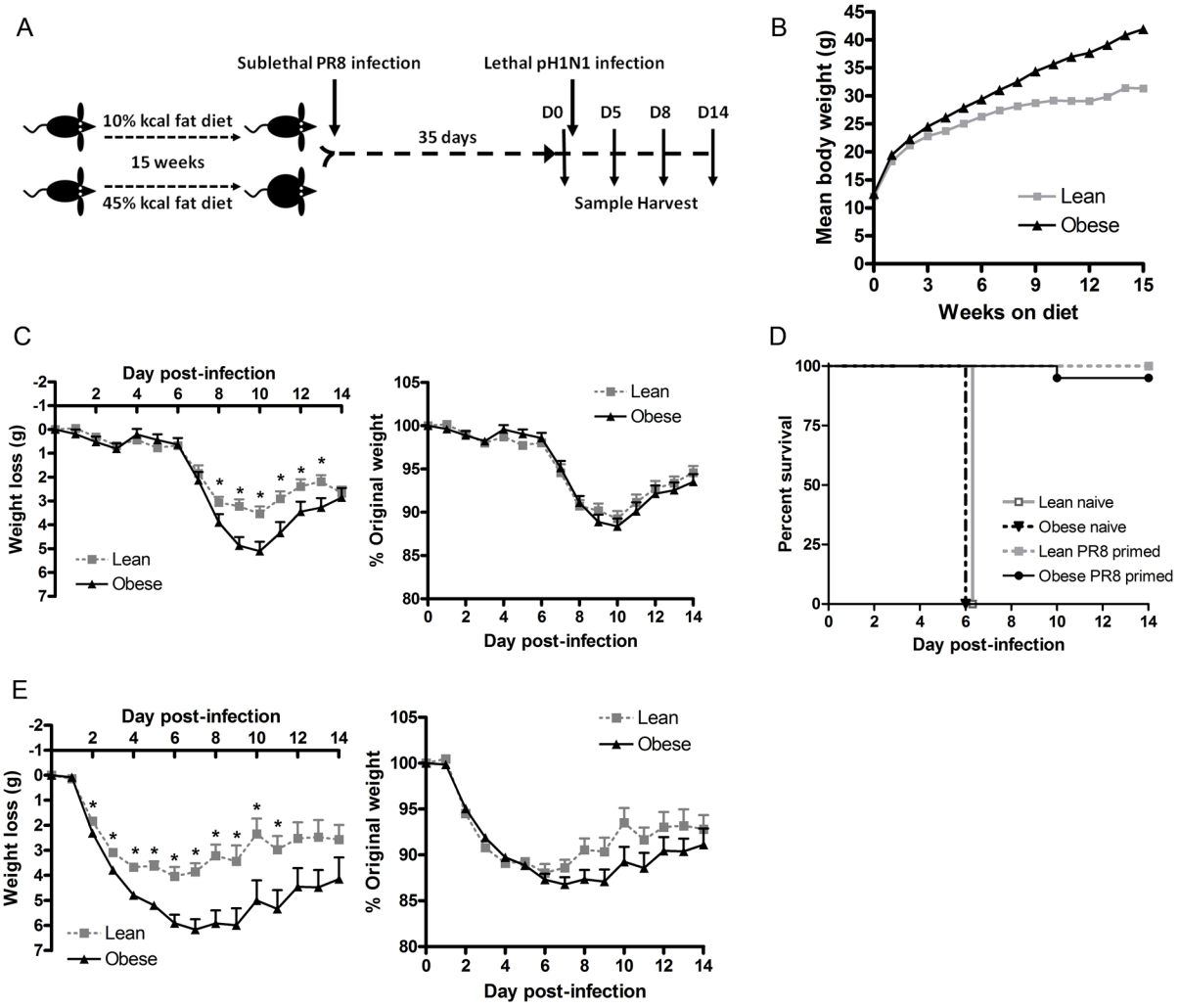

FIGURE 1.

A sublethal influenza A/PR/8/34 infection induces heterologous protection against a lethal pH1N1 challenge in lean and diet-induced obese mice. A, Weanling, male C57BL/6J mice were placed on a high fat or low fat, control diet for 15 wk. Lean and obese mice were infected with a sublethal dose of influenza A/PR/8/34. Thirty-five days after the primary infection, mice were challenged with a lethal dose of pH1N1 and samples were harvested at day 0 (naïve to pH1N1), and 5, 8 and 14 dpi. B, Mice fed a high fat diet gain significantly more weight than mice fed a low fat, control diet (n≥40 per group). After one week and throughout dietary exposure, high fat diet fed mice weigh significantly more than low fat diet fed mice. C, Fifteen weeks after mice were placed on the designated diets, mice were inoculated with a sublethal dose of PR8, and weight loss was monitored daily. D, Five weeks after the primary PR8 infection, PR8 primed (two cohorts of n=46) and naive mice (n=3–4) were challenged with a lethal dose of pH1N1. The naïve mice rapidly succumbed to the pH1N1 challenge, whereas primed mice did not. E, Secondary pH1N1 infection weight loss. Diet-induced weight gain graphs and infection weight loss graphs represent means ± SEM of at least two independent experiments. *p<0.05 compared with obese mice.

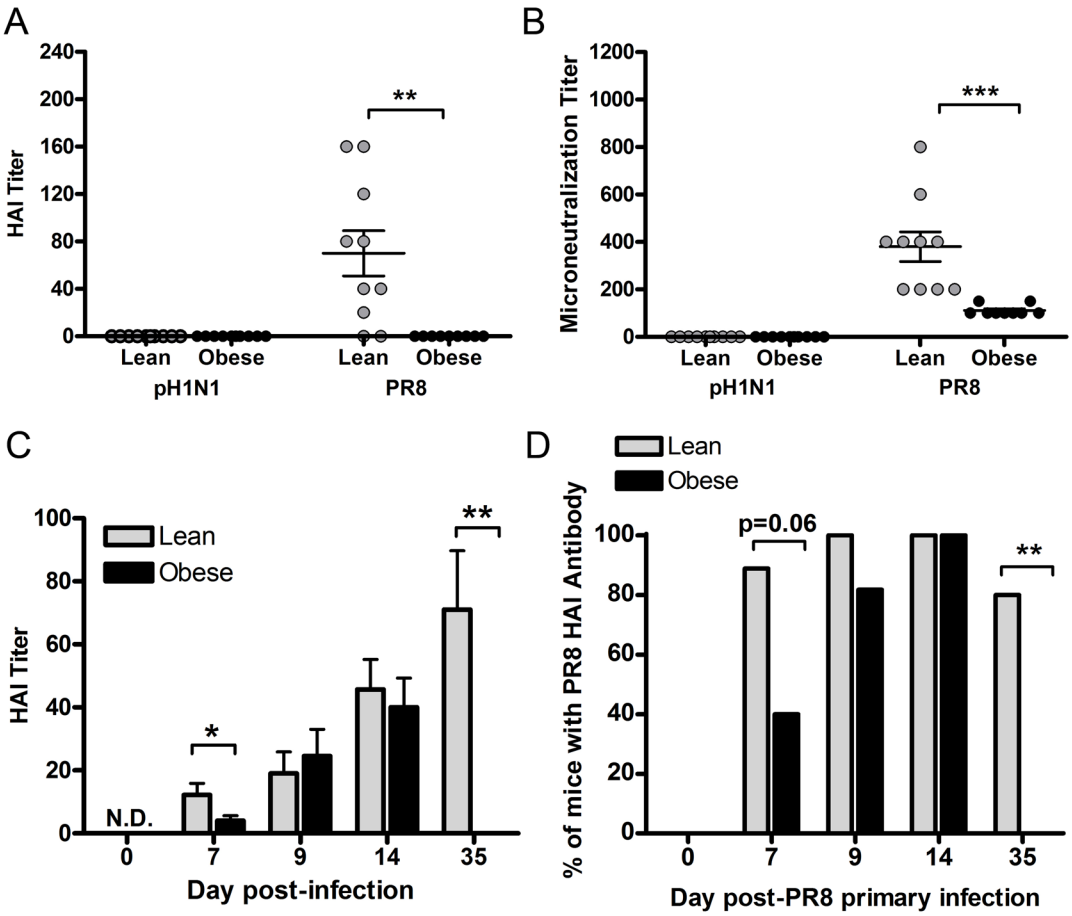

FIGURE 2.

Obese mice exhibit delayed antibody production and impaired antibody maintenance following a sublethal PR8 infection. A and B, HAI (A) and microneutralization (B) titers of sera from lean and obese mice 5 wk after a primary PR8 infection, demonstrating that PR8 does not elicit a cross-neutralizing pH1N1 antibody response (n=9–10). C and D, PR8 HAI titer (C) and percentage of mice with detectable PR8 HAI antibodies (D) following a sublethal PR8 infection (n=8–11). The limit of detection for HAI and microneutralization titers is 10. Each data point represents an individual animal. Bars represent mean HAI ± SEM or percentage of mice with detectable PR8 HAI. *p<0.05, **p<0.005, ***p<0.0005.

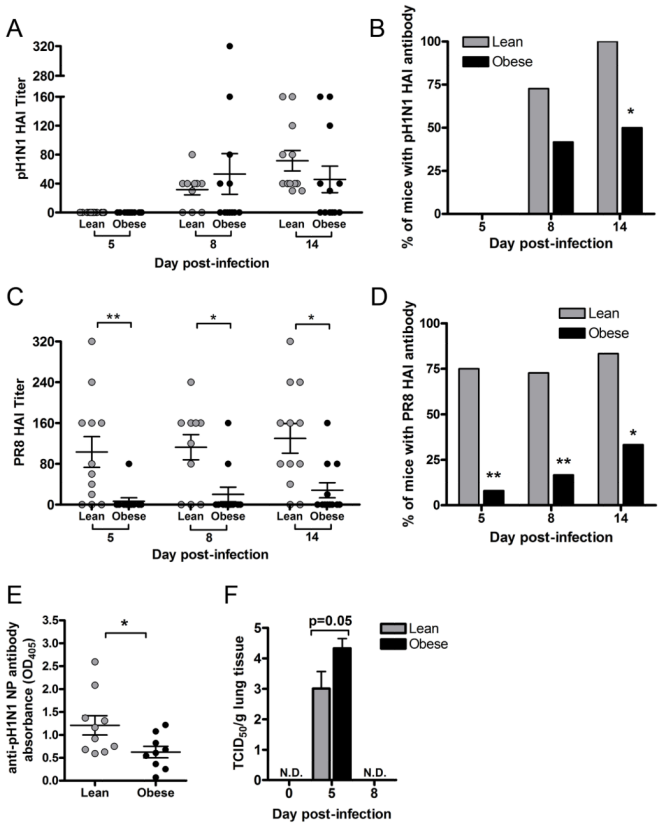

FIGURE 3.

Obese mice have lower levels of cross-reactive anti-pH1N1 nucleoprotein antibodies and exhibit greater lung viral titers during a secondary pH1N1 infection. A and B, Serum pH1N1 HAI titer (A) and percentage of mice with detectable pH1N1 HAI antibodies (B) during a secondary heterologous pH1N1 challenge, n=10–12. C and D, Serum PR8 HAI titer (C) and percentage of mice with detectable PR8 HAI antibodies (D) during a secondary heterologous pH1N1 challenge, n=10–12. The limit of detection for HAI titers is 10. E, Obese mice have lower levels of serum cross-reactive anti-pH1N1 NP antibodies 5 wk after a primary PR8 infection, n=9–10. F, Obese mice have a greater viral burden at 5 dpi during the pH1N1 rechallenge (n=12). No virus was detected (N.D.) at 0 or 8 dpi, n=5–6 at 0 and 8 dpi. Each data point represents an individual animal. Bars represent percentage of mice with detectable HAI antibody or mean viral titer ± SEM. *p<0.05, **p<0.005 compared with lean mice.

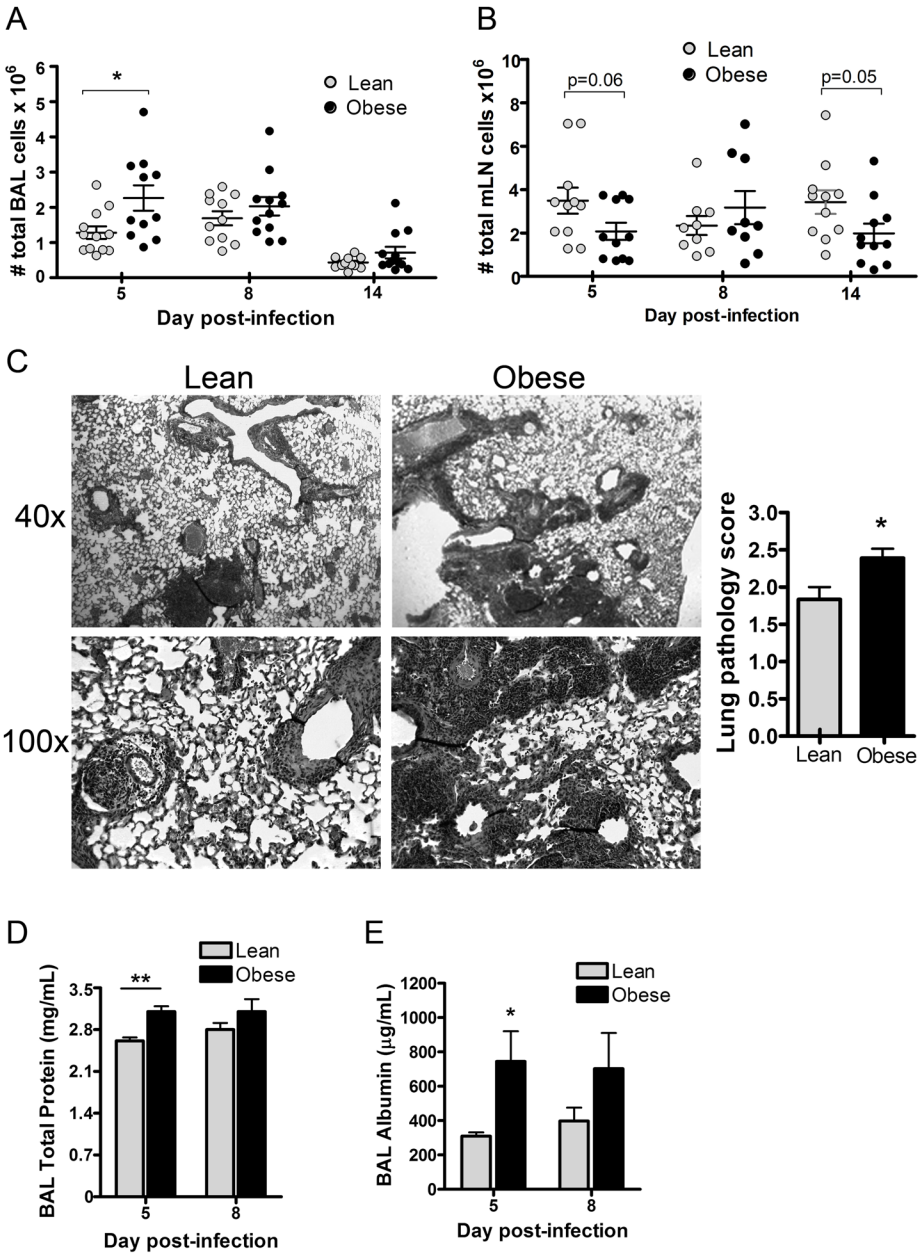

FIGURE 4.

Obese mice exhibit a greater inflammatory and pathological response in the lungs following a secondary heterologous pH1N1 challenge. A and B, Enumeration of BAL cells (A) and mLN cells (B) at 5, 8 and 14 dpi following the secondary pH1N1 challenge, n=9–12. Each data point represents an individual animal. C, Representative H&E stained lung histology slides at 40x and 100x magnification and pathology score at 5 dpi, n=3–4. D, Total protein in BAL fluid at 5 and 8 dpi, n=5–6. E, Albumin levels in BAL fluid at 5 and 8 dpi, n=5–6. Bars represent mean ± SEM, *p<0.05, **p<0.005 compared with lean mice.

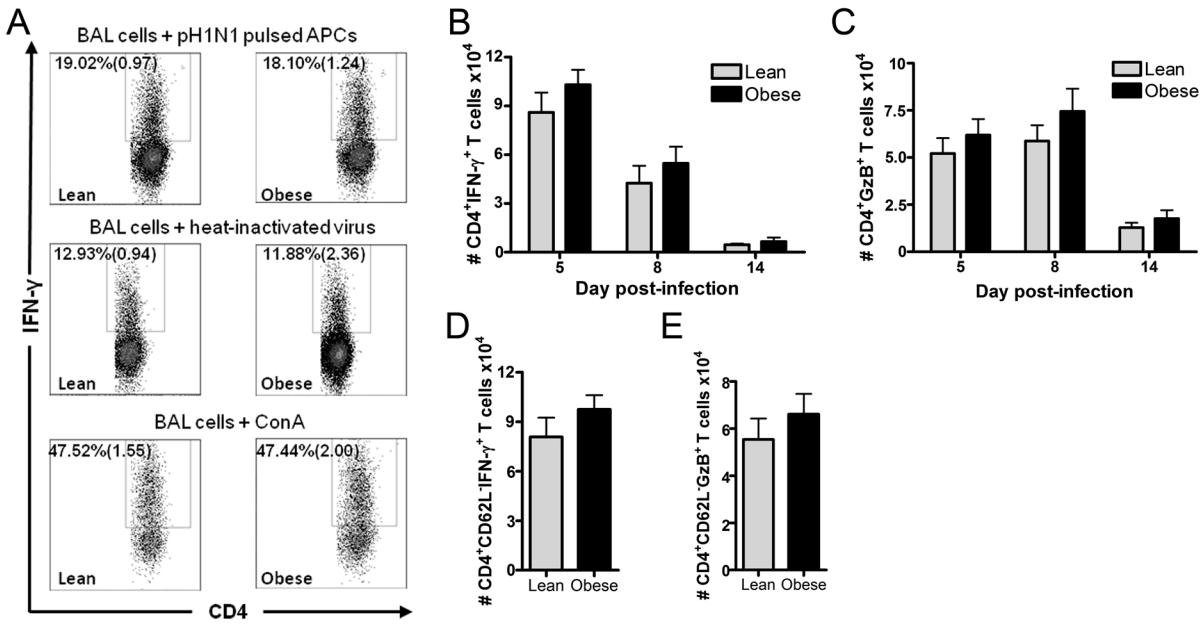

FIGURE 5.

Exposure to PR8 elicits a rapid and robust memory $CD4^+$ T-cell response following pH1N1 infection in both lean and obese mice. BAL cells from mice challenged with a secondary heterologous pH1N1 infection were stimulated for 6h with heat-inactivated pH1N1 (n=5–6), pH1N1 pulsed APCs (n=4–6) or Con A (n=5–6). A, Representative flow cytometry gating scheme at 5 dpi, including mean % (SEM). B and C, Number of IFN-γ (B) and GzB (C) producing $CD4^+$ T cells after stimulation with pH1N1 pulsed APCs, n=4–6. D and E, Number of IFN-γ (D) and GzB (E) producing effector memory $CD4^+$ T cells after stimulation with pH1N1 pulsed APCs at 5 dpi, n=4–6. Each bar represents the mean ± SEM.

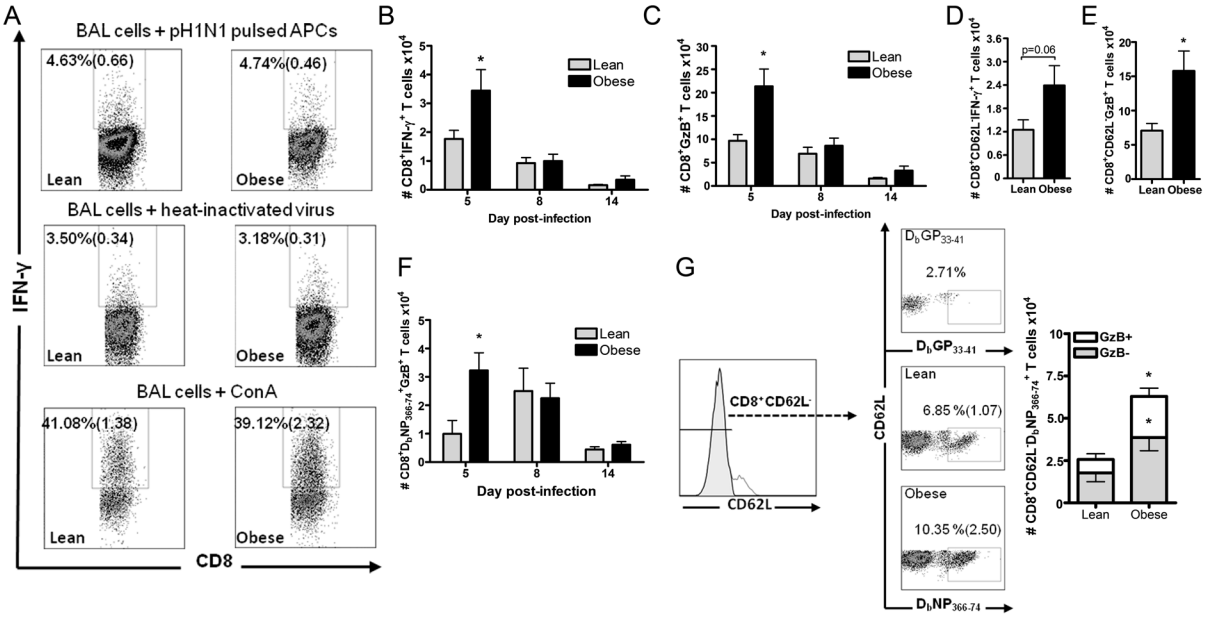

FIGURE 6.

Obese mice have enhanced cross-reactive $CD8^+$ T-cell responses at 5 dpi after a secondary heterologous pH1N1 challenge. A, BAL cells from mice challenged with a secondary heterologous pH1N1 infection were stimulated as described in the legend to Figure 4. A, Representative flow cytometry gating scheme at 5 dpi, including mean percentage (SEM), n=4–6. B and C, Number of IFN-γ (B) and GzB (C) producing $CD8^+$ T cells after stimulation with pH1N1 pulsed APCs, n=4–6. D and E, Number of IFN-γ (D) and GzB (E) producing effector memory $CD8^+$ T cells after stimulation with pH1N1 pulsed APCs at 5 dpi, n=4–6. F, Enumeration of GzB producing, NP_{366-74} specific $CD8^+$ T cells in the BAL compartment, n=4–6. G, Comparison of GzB production by NP-specific effector memory $CD8^+$ T cells stimulated with APCs at 5 dpi, n=4–6. Each bar represents the mean ± SEM, *$p<0.05$ compared with lean mice at 5 dpi.

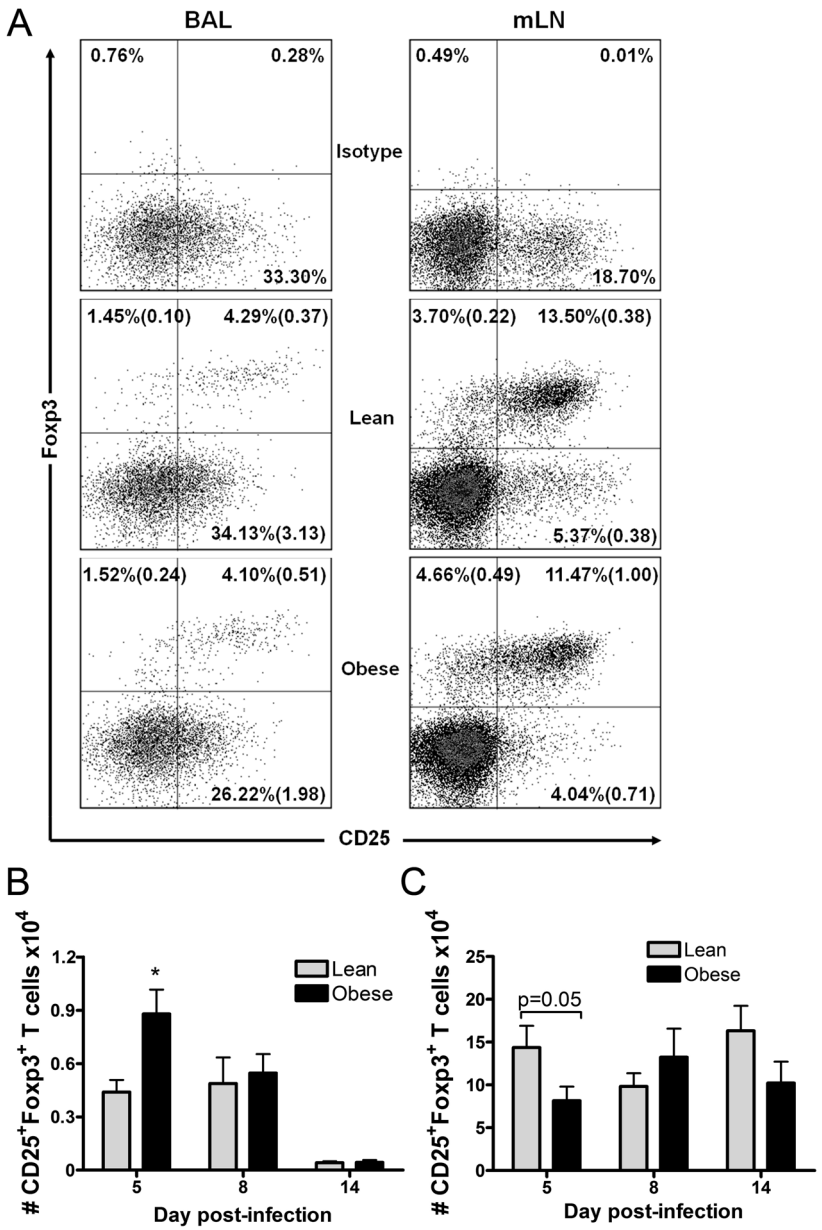

FIGURE 7.

Obese mice have a greater number of Tregs in the lung airways during a heterologous secondary pH1N1 challenge. A, Representative BAL (n=5–6) and mLN (n=10–12) $CD4^+CD25^+Foxp3^+$ Treg gating scheme at 5 dpi, including mean percentage (SEM). B and C, Enumeration of Tregs in BAL fluid (B) and mLN (C). Each bar represents the mean ± SEM, and *p<0.05 compared with lean mice at 5 dpi.

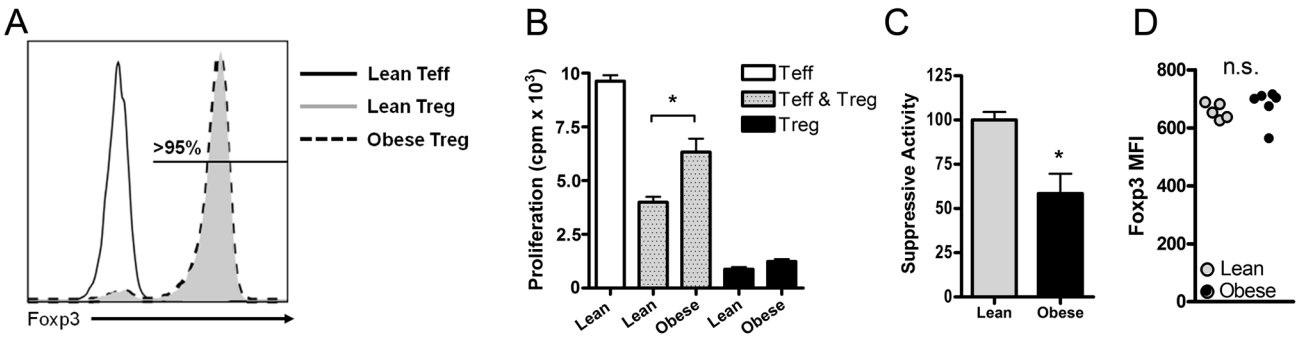

FIGURE 8.

Tregs isolated from obese mice are significantly less suppressive than Tregs isolated from lean mice. Pooled $CD4^+CD25^-$ Teff cells and $CD4^+CD25^+$ Tregs were isolated from splenocytes of naïve lean (n=3) and obese mice (n=3). A, Greater than 95% of isolated Tregs expressed Foxp3 from lean and obese mice, and less than 5% of Teff cells expressed Foxp3 as determined by FACS analysis, confirming pure populations of cells. B, Suppression assay comparing functionality of lean Tregs and obese Tregs cocultured with lean Teff cells at a ratio of 1:2 in the presence of anti-CD3/CD28 for 72 h. C, Normalized suppressive activity of isolated Tregs. D, Foxp3 median fluorescence intensity (MFI) of Tregs from splenocytes of lean and obese mice. Each data point represents an individual animal, n=5–6. Each bar represents the mean ± SEM, and *$p<0.05$ compared with lean mice.

Table I

Similar levels of lung cytokine and chemokine expression during a secondary heterologous pH1N1 challenge in lean and obese mice

Gene	Dietary Group[a]	Day 0	Day 5	Day 8	Day 14
TNF-α	*Lean*	1.00±0.11	1.92±0.44	0.89±0.12	1.12±0.10
	Obese	0.83±0.09	2.20±0.51*	0.78±0.09	0.84±0.12
IL-1β	*Lean*	1.00±0.11	1.75±0.29*	0.69±0.10	0.59±0.07*
	Obese	3.07±1.13	2.64±0.57	0.59±0.10*	0.53±0.08*
IFN-γ	*Lean*	1.00±0.32	6.33±0.69*	2.41±0.29*	1.96±0.10
	Obese	0.71±0.15	6.58±1.69*	2.01±0.19*	1.81±0.11*
IL-10	*Lean*	1.00±0.18	6.62±0.83*	2.84±0.29*	0.94±0.05
	Obese	1.11±0.34	8.31±5.09	4.09±0.69*	1.40±0.42
RANTES	*Lean*	1.00±0.51	0.69±0.08	1.08±0.20	0.64±0.20
	Obese	0.48±0.0.08	0.73±0.15	0.76±0.09	0.79±0.15
MCP-1	*Lean*	1.00±0.11	14.25±1.34*	1.32±0.18	0.77±0.05
	Obese	0.73±0.01	23.99±7.49*	2.20±0.83*	0.86±0.11

[a]Values represent mean fold increase over uninfected control ± SEM (n=4–6),

*$p<0.05$ compared with 0 dpi within same dietary group. There were no statistical differences between lean and obese mice at any time point